Charge Redistribution in Adenosylribosyl Transferase Caused by Substitution of a Single Amino Acid Residue

Mary Gianniosis[a], Valerio Berardi[b], Adalberto Bonincontro[c], Eric Dabbs[a], and Gianfranco Risuleo[b,c,*]

[a] School of Molecular and Cell Biology, University of Witwatersrand, Johannesburg, South Africa
[b] Dipartimento di Genetica e Biologia Molecolare, Università di Roma "La Sapienza", P. le A. Moro, 5, I-00185 Roma, Italy
[c] CNISM and SOFT-INFM-CNR Research Center, Dipartimento di Fisica, Università di Roma "La Sapienza", P. le A. Moro, 5, I-00185 Roma, Italy. E-mail: gianfranco.risuleo@uniroma1.it

* Author for correspondence and reprint requests

Z. Naturforsch. **63c**, 889–892 (2008); received March 28/May 13, 2008

Dielectric measurements in the frequency range 10^5–10^8 Hz were performed on wild-type (wt) adenosylribosyl transferase and a mutant enzyme. The analysis of the dielectric relaxation curve allowed the estimation of the hydrodynamic radius and of the electric dipole moment. The first parameter remained unchanged in wt and mutant protein. The dipole moment of the mutant, however, was significantly increased. Implications on the electrostatic interactions between enzyme and substrate are discussed.

Key words: Adenosylribosyl Transferase, Dielectric Spectroscopy, Protein Structure

Introduction

Rifamycins are the principal group of antimicrobials which inhibit prokaryotic transcription and are extensively used to combat *Mycobacterium tuberculosis* infections (Woodley *et al*., 1972). This group consists of a number of related compounds biosynthesized by *Amycolatopsis mediterranei* (Lancini and Parenti, 1978); the genes responsible were cloned and characterized (Schupp *et al*., 1998; Tang *et al*., 1998). These natural products have been modified to enhance efficacy: rifampicin is the most widely used, but other examples are rifabutin, rifapentene, and rifamixin (Sensi, 1983). Rifampicin binds to the DNA-dependent RNA polymerase and blocks the elongation of the RNA (Wehrli and Staehelin, 1971). Another response to rifampicin in mycobacteria and related species is its inactivation, the drug being decomposed (Dabbs, 1991). Subsequently, two additional inactivation mechanisms were identified: glucosylation by *Nocardia brasiliensis* (Yazawa *et al*., 1993) and phosphorylation by *Nocardia otitidiscaviarum* (Yazawa *et al*., 1994). Another mechanism, ribosylation, was first observed in *Mycobacterium smegmatis*. It was shown that this ribosylation consisted of a two-step biochemical reaction after the initial formation of an ADP-ribosylated drug (Dabbs *et al*., 1995). The ADP-ribosyl transferase (*arr*) enzyme consists of 143 amino acid residues and is unusually thermostable (Quan *et al*., 1997), although highly photosensitive. Disruption of the *arr* gene in *M. smegmatis* resulted in susceptibility increasing by 12- to 15-fold, showing that this gene product does contribute to the quite high *in vivo* rifampicin MIC (Dabbs and Quan, 2000).

Considering the relatively little knowledge about the chemico-physical properties of this protein, so important in antibiotic inactivation, we decided to gain an insight into this particular aspect adopting a well established biophysical approach. This is based on dielectric spectroscopy which provides information on the conformational structure of the protein and on protein-nucleic acid interactions (Bonincontro and Risuleo, 2003, 2005).

Experimental

Error-prone PCR mutagenesis

PCR was performed in a MJ MINI™ thermal cycler (Bio-Rad Laboratories Ltd., Johannesburg, South Africa). The template was the *arr* ORF,

While this manuscript was processed an interesting article related to Arr structure and diversity was published by Baysarowich J. (2008), Proc. Natl. Acad. Sci. USA **105**, 4886–4891.

cloned into pGEM3Z(f-) (Promega Corporation, Madison, WI, USA). The reaction utilized 5′-GTGGTGGCGAATCCGCCGAAA-3′ and 5′-CTAGTCATAGATGACCGCGAG-3′ as the forward and reverse primers, respectively. Mutagenic PCR was used to introduce random point mutations into the *arr* ORF. The amplification product was subjected to agarose gel electrophoresis to verify the fragment of interest. The amplified fragments were cloned into pGEM-T-Easy (Qiagen, Cape Town, South Africa) and tested for reduced rifampicin MIC in *E. coli* DH5α.

Protein purification

The culture (100 ml) was centrifuged, and the resulted pellet re-suspended in 1 ml lysis buffer [50 mM NaH_2PO_4, 300 mM NaCl, 10 mM imidazole, lysozyme (1 mg/ml final concentration)] and incubated on ice for 30 min. Cells were broken by sonic vibration (VCX 600 Vibra Cell, Sonics and Materials, Inc., Newtown, CT, USA) for 10 s (6 cycles) with 5 s intervals. The lysate was centrifuged at $3 \cdot 10^4 \times g$ for 25 min at 4 °C. The supernatant (600 μl) was applied to Ni-NTA spin columns equilibrated with 600 μl of lysis buffer. The cleared lysate contained the 6×His-tagged protein. The columns were microfuged for 4 min at $2 \cdot 10^3 \times g$ for 4 min. The eluate was collected and columns were washed three times with 600 μl of wash buffer (50 mM NaH_2PO_4, 300 mM NaCl, 20 mM imidazole). The wash fractions were analyzed by SDS-PAGE to ascertain the stringency of the wash. The fusion protein was eluted twice with 100 μl of elution buffer (50 mM NaH_2PO_4, 300 mM NaCl, 250 mM imidazole) after centrifugation at $2 \cdot 10^3 \times g$ for 2 min.

Dielectric spectroscopy

The apparatus was a computer-controlled HP impedance analyzer, Mod. 4194A, working in the 0.1–100 MHz range. The measuring cell was previously described (Bonincontro *et al.*, 1996) and calibrated according to standard procedures (Athey *et al.*, 1982). The errors on the real, ε', and the imaginary part, ε'', of the complex dielectric constant, ε, were within 1% and 3%, respectively. The dielectric relaxation loss, ε_d'', was obtained subtracting the ionic contribution, $\chi/\varepsilon_0\omega$, where χ is the sample conductivity, ω the angular frequency of the applied electric field and ε_0 the vacuum dielectric constant. The cell was thermally controlled to (20.0 ± 0.1) °C.

Results and Discussion

We used the polymerase chain reaction (PCR) as modified by Cadwell and Joyce (1992). This approach exploits the elevated error rate of Taq polymerase in the presence of high concentration of $MgCl_2$ (10 mM) without significantly decreasing the level of amplification. Additionally, 0.5 mM $MnCl_2$ was added to the reaction mixture. Thirty amplification cycles were carried out resulting in the amplification of a region of the adenosyl-ribosyl transferase gene encompassing 432 bp. Fig. 1 shows the results of the mutagenesis. The mutation was assessed by restriction site destruction and resulted in the transversion *C*CG → *A*CG at nucleotide position 16 leading to a proline → threonine amino acid substitution. The chemical nature of the two amino acid residues is significantly different. Therefore one could expect significant structure alterations deriving from this amino acid

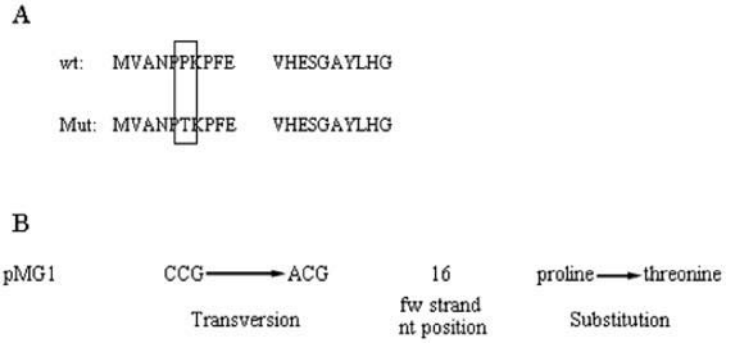

Fig. 1. (A) Wild-type (wt) and (B) mutant (Mut) amino acid sequences. The proline-threonine substitution is evidenced as well as the DNA transversion. The mutation was ascertained by destruction of the restriction site.

change. As a matter of fact both amino acids are chiral, but the proline side chain is constituted by a closed ring formed by three $-CH_2$ groups linking the α-C to the N atom in the amino group. Threonine, on the other hand, has an aliphatic side chain containing an $-OH$ group. Interestingly, this hydroxy group may be modified by glucosylation. This side-chain modification is involved in rifampicin de-toxification in two different bacteria of the *Nocardia* genus (Yazawa *et al.*, 1993, 1994). It should be noted, however, that the amino acid substitution caused in our mutant did not result in a reduced rifampicin MIC in *E. coli* DH5α (not shown).

The hypothesis, that mutagenesis may result in a structural alteration of the enzyme, was probed by dielectric spectroscopy, a strategy successfully used in our laboratory to investigate biomacromolecules (Bonincontro and Risuleo, 2003, 2005). Fig. 2 shows the result of the dielectric measurements performed on wild-type (wt) and pMG1 mutant protein in solution.

Data were fitted with the real part and imaginary part of the Cole-Cole equation

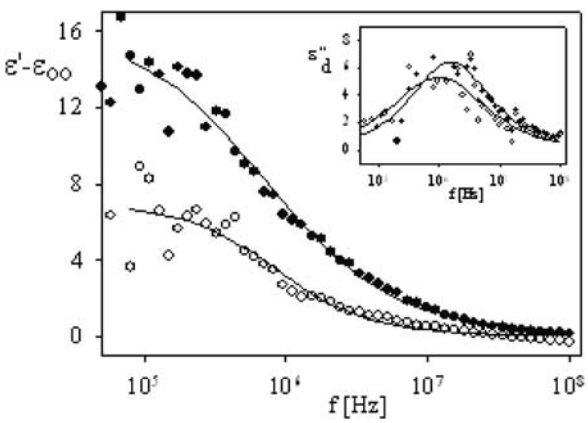

Fig. 2. Dielectric dispersion of protein suspensions at 20.0 °C. Data are reported as $\varepsilon' - \varepsilon_\infty$ vs. f, in Hz, in semi-logarithmic scale. Circles, wild-type protein; dots, mutant protein. In the inset the respective imaginary spectra are reported.

$$\varepsilon = \varepsilon_\infty + \frac{\Delta\varepsilon}{1 + \left(\mathrm{i}\frac{f}{f^*}\right)^{(1-\alpha)}} \quad , \tag{1}$$

where ε is the complex dielectric constant, f is the measuring frequency, f^* is the relaxation frequency, i is the imaginary unit, $\Delta\varepsilon$ is the dielectric increment, ε_∞ is the value of ε' extrapolated at high frequency, and α is an empirical parameter taking into account a spread of relaxation times (Hasted, 1973). The electric dipole moment, μ, of the protein was estimated from the dielectric increment, $\Delta\varepsilon$, using the Oncley formula

$$\mu^2 = \frac{2\varepsilon_0 MkT\Delta\varepsilon}{Ncg} \quad , \tag{2}$$

where M is the protein molecular mass expressed in kDa, T is the temperature expressed in K, while k is the Boltzmann constant, ε_0 is the vacuum dielectric constant, N is the Avogadro number, c is the protein concentration expressed in mg/ml, and g is the molecular correlation parameter generally assumed as unit factor in dilute protein solutions (Pethig, 1979; Pethig and Kell, 1987).

The effective hydrodynamic radius, r, of the protein was calculated from the relaxation frequency, f^*, using the equation

$$f^* = \frac{kT}{8\pi^2\eta r^3} \quad , \tag{3}$$

where η is the viscosity of the solvent (Grant *et al.*, 1978).

The results of this analysis are reported in Table I. The estimated hydrodynamic radius for the wt enzyme appears rather large for a globular protein of this molecular weight. For instance, lysozyme with a comparable molecular weight has a hydrodynamic radius of 2 nm. This means that the rota-

Table I. Results of the Cole-Cole best fit of the experimental data. The concentration, the calculated apparent hydrodynamic radius and electric dipole moment are also presented. pGM1 is the recombinant plasmid encoding the mutant DNA sequence.

Sample	c [mg/ml]	$\Delta\varepsilon$	f^* [MHz]	α	r [nm]	μ [D]
Wild-type	1.83	7.0 ± 0.8	0.72 ± 0.09	0.17 ± 0.09	4.1 ± 0.2	810 ± 40
pMG1	1.35	16 ± 2	0.8 ± 0.1	0.30 ± 0.04	4.0 ± 0.2	1420 ± 70

tional coefficient of diffusion is influenced by a form factor, which suggests a pronounced elongated shape for the three-dimensional conformation of the protein. In the mutant *arr* enzyme this conformational parameter does not seem to be affected. On the other hand, the dipole moment is significantly modified. As a matter of fact, the pattern of the relaxation curve clearly shows that the mutant protein has a much higher dielectric increment as compared to the wt enzyme. The dielectric increment is proportional to the concentration. Since the concentration of the mutant protein is lower, the actual effect on $\Delta\varepsilon$ is much higher in reality. The value of μ in the mutant increases by about 75% (see Table I). Considering that the estimated hydrodynamic radius is almost constant, the variation of the dipole moment must be attributed exclusively to a drastic redistribution of the surface charges. The increase of the dipole moment is consistent with a significantly higher physical separation of the electric charges.

In conclusion, in this short communication we presented evidence of a significant structural alteration of the *arr* protein. The dramatic charge redistribution, as demonstrated by dielectric spectroscopy, is due to a single amino acid substitution which apparently does not affect the enzyme-substrate interaction. The results presented here could be of significance for investigators of the mechanisms of drug inactivation mediated by this enzyme.

Acknowledgements

E. D. and G. R. obtained a traveling grant for an exchange program from the National Research Foundation (South Africa) and the Ministry of Foreign Affairs (Italy).

Athey T. W., Stuckly M. A., and Stuckly S. S. (1982), Measurement of radio frequency permittivity of biological tissues with an open-ended coaxial line: Part I. IEEE Trans. **30**, 82–86.

Bonincontro A. and Risuleo G. (2003), Dielectric spectroscopy as a probe for the investigation of conformational properties of proteins. Spectrochim. Acta A: Mol. Biomol. Spectrosc. **59**, 2677–2684.

Bonincontro A. and Risuleo G. (2005), Structural studies of *E. coli* ribosomes by spectroscopic techniques: a specialized review. Spectrochim. Acta A: Mol. Biomol. Spectrosc. **62**, 1070–1080.

Bonincontro A., Briganti G., Giansanti A., Pedone F., and Risuleo G. (1996), Electrical conductivity and dielectric dispersion of *E. coli* ribosomes and of 30S and 50S ribosomal subunits: effect of magnesium ions. Colloids Surf. B: Biointerfaces **6**, 219–223.

Cadwell R. C. and Joyce R. F. (1992), Randomization of genes by PCR mutagenesis. PCR Methods Appl. **2**, 28–33.

Dabbs E. R. (1991), Cloning of nocardioform DNA conferring the ability to inactivate rifampicin. FEMS Microbiol. Lett. **63**, 247–250.

Dabbs E. R. and Quan S. (2000), Light inhibits rifampicin inactivation and reduces rifampicin resistance due to a cloned mycobacterial ADP-ribosylation gene. FEMS Microbiol. Lett. **182**, 105–109.

Dabbs E. R., Yazawa K., Mikami Y., Miyaji M., Morisaki N., Iwasaki S., and Furihata K. (1995), Ribosylation by mycobacterial strains as a new mechanism of rifampin inactivation. Antimicrob. Agents Chemother. **39**, 1007–1009.

Grant E. H., Sheppard R. J., and South G. P. (1978), Dielectric Behavior of Biological Molecules in Solution. Clarendon, Oxford.

Hasted J. B. (1973), Aqueous Dielectrics. Chapman & Hall, London.

Lancini G. C. and Parenti F. (1978), Rifamycin biogenesis. In: Antibiotics and Other Secondary Metabolites Biosynthesis and Production (Hütter R., Leisinger T., Nüesch J., and Wehrli W., eds.). Academic Press, London, pp. 129–139.

Pethig R. (1979), Dielectric and Electronic Properties of Biological Materials. Wiley, New York.

Pethig R. and Kell D. B. (1987), The passive electrical properties of biological systems: Their significance in physiology, biophysics and biotechnology. Phys. Med. Biol. **32**, 933–970.

Quan S., Venter H., and Dabbs E. R. (1997), Ribosylative inactivation of rifampin by *Mycobacterium smegmatis* is a principal contributor to its low susceptibility to this antibiotic. Antimicrob. Agents Chemother. **41**, 2456–2460.

Schupp T., Toupet C., Engel N., and Goff S. (1998), Cloning and sequence analysis of the putative rifamycin polyketide synthase gene cluster from *Amycolatopsis mediterranei*. FEMS Microbiol. Lett. **159**, 201–207

Sensi P. (1983), History of the development of rifampin. Rev. Infect. Dis. **5**, 402–406.

Tang L., Yoon Y. J., Choi C. Y., and Hutchinson C. R. (1998), Characterization of the enzymatic domains in the modular polyketide synthase involved in rifamycin B biosynthesis by *Amycolatopsis mediterranei*. Gene **216**, 255–265.

Wehrli W. and Staehelin M. (1971), Actions of the rifamycins. Bact. Rev. **35**, 290–308.

Woodley C. L., Kilburn J. O., David H. L., and Silcox V. A. (1972), Susceptibility of mycobacteria to rifampin. Antimicrob. Agents Chemother. **2**, 245–249.

Yazawa K., Mikami Y., Maeda N., Akao M., Morisaki N., and Iwasaki S. (1993), Inactivation of rifampin by *Nocardia brasiliensis*. Antimicrob. Agents Chemother. **37**, 1313–1317.

Yazawa K., Mikami Y., Maeda A., Morisaki N., and Iwasaki S. (1994), Phosphorylative inactivation of rifampicin by *Nocardia otitidiscaviarum*. J. Antimicrob. Chemother. **33**, 1127–1135.